EXPERIMENTAL AND NUMERICAL STUDY OF TEMPERATURE FIELD DURING HARD-FACING OF DIFFERENT CARBON STEELS

by

Dušan M. ARSIĆ[a*], Ivana B. IVANOVIĆ[b], Aleksandar S. SEDMAK[c], Mirjana M. LAZIĆ[d], Dragan V. KALABA[e], Ivana R. ČEKOVIĆ[b], and Nada R. RATKOVIĆ[a]

[a] Faculty of Engineering, University of Kragujevac, Kragujevac, Serbia
[b] Innovation Center, Faculty of Mechanical Engineering, University of Belgrade, Belgrade, Serbia
[c] Faculty of Mechanical Engineering, University of Belgrade, Belgrade, Serbia
[d] Faculty of Science, University of Kragujevac, Kragujevac, Serbia
[e] Faculty of Technical Sciences, University of Priština, Kosovska Mitrovica, Serbia

Original scientific paper
https://doi.org/10.2298/TSCI190717338A

In this research the 3-D transient non-linear thermal analysis of the hard-facing process was performed by using the experimental testing and finite element method. Testing was done at three different carbon steels and the obtained results were compared to one obtained by empirical formulas and welding recommendations. Experimental testing was done on hard faced specimens (plates) with different thickness. Temperatures and temperature cycles was measured by using thermocouples in order to determine maximal temperature and cooling time between 800 ºC and 500 ºC. After experimental testing the finite element method analysis was done. The simulations were executed on the open source platform Salome using the open source finite element solver Code Aster. The Gaussian double ellipsoid was selected in order to enable greater possibilities for the calculation of the moving heat source. The numerical results were compared with available experimental and mathematical results.

Key words: *temperature cycles, welding simulations, transient heat conduction, moving heat source*

Introduction

Hard facing represents process of deposition of molten material to the other material called substrate. Mostly used hard facing methods are conventional welding methods such as MMA, GMA or TIG [1-4], although today are in use and some modern methods [5]. Hard facing is mostly used for reparation of damaged parts when due to damage they cannot be used properly to retrieve its working function [4-7]. Thereby application of these technologies can lead to numerous savings [8]. Hard facing can be compared to welding, so all welding parameters such as: preheating temperature, welding regimes, temperature cycles, heat treatment, *etc*. can affect properties of base material and hard facing (weld metal). Here the calculation of the cooling time between 800 ºC and 500 ºC has to be emphasized, so as such its significance was already analyzed in many previous publications [1, 9-14]. In that researches it was determined that the most critical zone for the creation of brittle and unwanted structures is right bellow

* Corresponding author, e-mail: dusan.arsic@fink.rs

hard faced layer. In order to better understanding the complexity of the problem, temperature cycle bellow hard faced layer need to be determined. Temperature cycle can be determined experimentally and numerically. Experimental determination of temperature cycle is the most reliable and can be done by using thermocouples while numerical methods are based on finite element methods (FEM) and creation of model identical to the real one. Obtained results are than compared to experimental in order to determine matching level [15]. This paper is aimed to emphasize possibilities for numerical calculation of temperature cycles during hard facing of different carbon steels, as well as to show its accuracy compared to the experimental results.

From the aspect of FEM, the hard-facing process belongs to a group of welding problems which are usually simulated as 3-D transient heat transfer problems. Also, if the thermal properties of the material are treated as temperature dependent, problem is referred as non-linear. The most important issue of numerical model is the moving heat source. It can be said that numerical simulation of the hard-facing process is a great simplification of the real process. The model is most often a plate with the heat source moving along one axis with constant velocity. Creation of model need to be done very careful since otherwise there is no guarantee that results will be results. For a long time, numerous experimental and numerical studies have been dealing with different aspects of the problem [9, 15-24]. There is a wide range of functions for the heat source implementation, but the most accepted is certainly the double ellipsoidal heat source [24, 25]. Recently, those studies dealing with a reliability of both, experimental and numerical results have become significant [10, 15, 26-31]. Also, it should be emphasized that inappropriate thermal conditions during welding or hard facing can cause crack occurrence at structures [32-35].

The model for this numerical analysis was a plate that was chosen from a very extensive experimental analysis of the hard-facing process similar researches given in [1, 2, 10]. During selection priority was given to a group of measurements that provide most information for the set-up of the numerical model and for the validation of numerical results. The initial idea was to ensure as accurate is possible numerical results of the temperature field that would be used for the future mechanical analysis of the same model. If the model proves to be accurate, in some further investigations experimental procedure can be avoided.

Experimental and numerical set-up

The models are two plates selected from a series of set-ups used for experimental analysis in [1, 2, 14]. The plates are made of different class carbon steels: C15, C35, C45, C45E and one wide used structural steel S355JR [36]. Plates were thick 10, 20, and 30 mm while the lengths and widths of the half plates were the same 430 and 200 mm, respectively. Thickness of the plates made of steels C15, C45E and S355JR were 10 mm, C35 was 30 mm, and C45 was made from 20 mm thick plate.

After the experimental procedure, numerical simulations were performed for two different heat sources, to simulate real conditions (as in experimental analysis [31]), with the characteristics listed in tab. 1.

The experimental results for the point in the symmetry plane, at 4 mm below the top surface, for five cases that were selected for numerical analysis, are presented in tab. 2. In the

Table 1. Characteristics of heat sources used for experimental measurements

Electrode diameter, d_e, [mm]	Welding voltage, U, [V]	Welding current, I, [A]	Welding velocity, v_s, [cms^{-1}]	Heat input, q_l, [Jcm^{-1}]
4.0	25.6	140	0.162-0.136	17650-21101
5.0	28.5	210	0.286-0.098	16736-48610

Table 2. Experimental results for carbon steels

No.	Electrode diameter, d_e, [mm]	Heat input, q_l, [Jcm^{-1}]	Initial temperature, T_0, [ºC]	Maximal temperature, T_{max}, [ºC]	Cooling time from 800 to 500ºC calculated according to different sources, $t_{8/5}$ [s]*				Base materials designation
					$(t_{8/5})^J$	$(t_{8/5})^{Sgr}$	$(t_{8/5})^R$	$(t_{8/5})^{EXP}$	
1	4.00	20082	20	875	19.6	57.7	31.0	20.5	C15
2	5.00	38667	97	1021	23.0	36.4	16.2	19.0	C35
3	5.00	48610	20	1145	28.3	76.7	49.5	28.0	C45
4	4.00	18200	20	833	16.9	47.4	26.8	15.5	C45E
5	5.00	16736	96	813	19.7	61.1	34.0	20.5	S355JR

* Formulas used for calculation of cooling time are in details given in [10]. Abbreviations are as follows: J – Japanese authors Ito and Bessyo, Sgr – expressions for limiting thickness, R – Rikallin´s expression, and EXP – experimental results.

table are given maximal values of temperature in the heat affected zone, measured at a point located below the top surface of the plate in the symmetry plane as well.

Experimental set-up is shown in fig. 1.

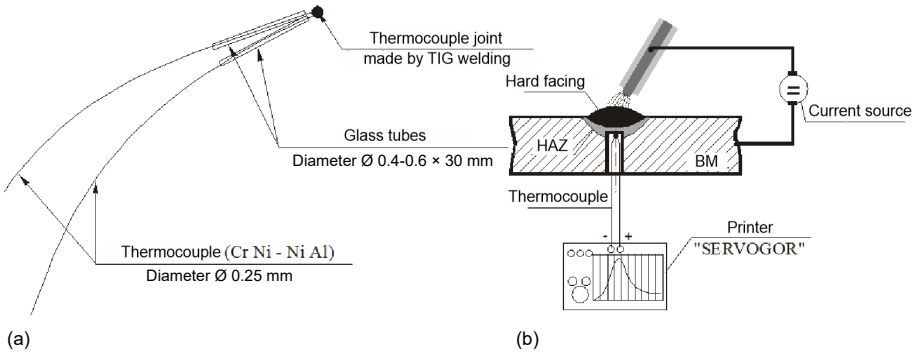

Figure. 1. Scheme of thermocouples (a) and measuring technique (b)

Numerical solution

The geometry of the model used in numerical simulations is a well-known half plate model. This model is usually chosen since the temperature field can be treated symmetrically with respect to the path of the heat source moving along one axis with constant velocity. Here, the heat source was moving with a constant velocity along the axis, the top half-surface was placed in the *x-y* plane, and the symmetry plane coincides with the *x-z* plane.

Calculations were performed on the open source Salome platform using the open source finite element solver Code Aster [37]. The thermal problem has been simulated as 3-D transient and also non-linear as thermal properties are temperature dependent. Besides the symmetry plane where the zero-flux condition was imposed at the boundary, at all other surfaces convection boundary conditions were imposed outside the influence of the heat source. For the volumetric heat source, the Gaussian double ellipsoid was used [28]. When the heat source is moving along the *x*-axis the double ellipsoid is given by the following expression:

$$q(x,y,z,t)=\frac{6\sqrt{3}fQ}{abc\pi\sqrt{\pi}}\mathrm{e}^{-3[x-(x_0+v_st)]^2/a^2}\mathrm{e}^{-3y2/b^2}\mathrm{e}^{-3z^2/c^2} \tag{1}$$

where Q is the power, v_s – the velocity, and x_0 – the initial position of the heat source.

Parameters a, b, and c in eq. (1) are the semi-axis of the ellipsoid. Since it is a double ellipsoid, the front and rear values of parameter a are different, as well as front and rear values of parameter f:

$$f_{\mathrm{f}} = \frac{2a_f}{a_f + a_r} \quad \text{and} \quad f_{\mathrm{r}} = 2 - f_{\mathrm{f}}$$

Results and discussions

Calculations were performed on a desktop PC with Intel Core i5-6400 CPU on 2.7 GHz and 32 GB RAM memory. The initial position of the heat source was placed at x equal to 6 mm. The heat transfer coefficient of 10 W/m^2°C was selected at convection boundaries. The time step was chosen to ensure approximately three calculation steps between two grid points.

For two cases from tab. 2 where electrodes of 4 mm diameter were used, the thickness of the plates was 10 mm and the initial temperature was the ambient temperature of 20 °C. After calibration, the semi-axes of the double ellipsoid were selected as follows: $c = 1.5$, $a_{\mathrm{f}} = a_{\mathrm{r}} = b = 10$. The results for the first case from this group, tab. 2, No. 1, are presented in fig. 2.

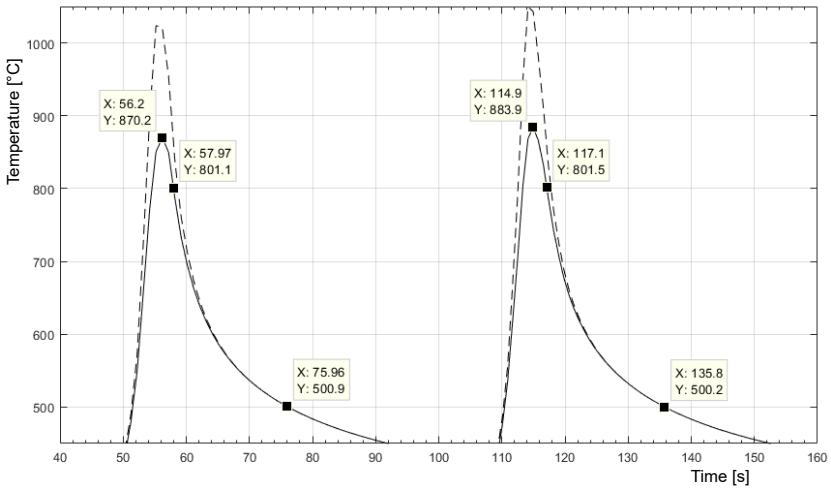

Figure 2. Numerical results for the temperature as a function of time from 450 °C for the point in the symmetry plane ($y = 0$), at $x = 0.1$ m, $x = 0.2$ m, and $z = 0.003$ m and 0.004 m (heat input 20082 J/cm, electrode diameter 4 mm)

At all shown diagrams, figs. 2-6, full line represents numerical solution for the temperature cycle while dashed line represents experimental curve.

For the selected heat source velocity of 0.0017 m/s, the maximal temperature at 4 mm under the top surface, at the distance 0.1 m from the top of the plate, is around 5 °C lower than the temperature obtained experimentally (875 °C). The cooling time from 800-500 °C is around 18 seconds which is 2 seconds lower than the experimental cooling time and 1.6 seconds lower than the time obtained from the Japanese authors formula, tab. 2. At the distance 0.2 from the top of the plate, the constant temperature has been reached. The maximal temperature at this point is higher than the experimental one but the cooling time is closer to experimental results.

The second case from the group, tab. 2, No. 4, is presented in fig. 3. The selected velocity of the heat source was 0.0019 m/s. Maximal temperature obtained numerically is 20 and more °C higher than experimentally obtained temperature but the cooling time is exactly the same as experimental cooling time.

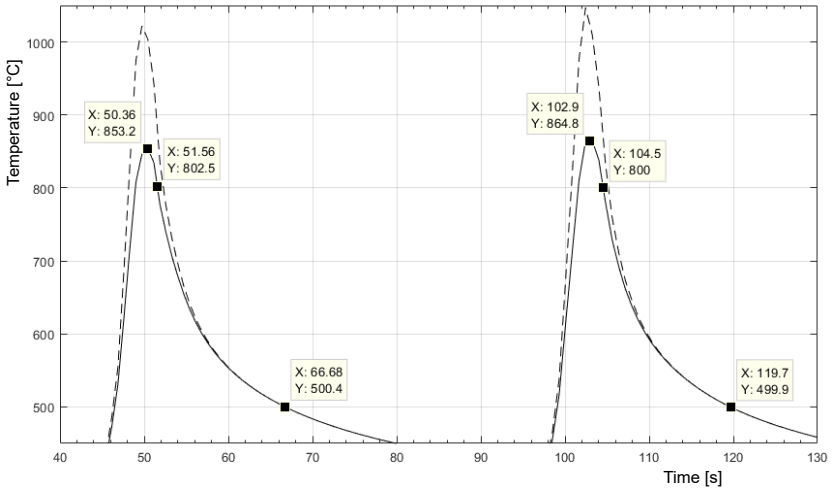

Figure 3. Numerical results for the temperature as a function of time from 450 °C for the point in the symmetry plane (y = 0), at x = 0.1 m, x = 0.2 m, and z = 0.003 m and 0.004 m (heat input 18200 J/cm, electrode diameter 4 mm)

For the electrode of 5 mm diameter, the calibration of the heat source was repeated, the values of c = 1.5 has remained unchanged while the other values are increased: $a_f = a_r = b =$ = 15. In the first example, tab. 1, No. 5, plate thickness was 10 mm and the initial temperature was 96 °C. Selected velocity for numerical simulation presented in fig. 4 was 0.0019 m/s.

It would be expected that the velocity of the heat source would be around 0.002 m/s but simulations with values above 0.0019 m/s resulted in much smaller cooling time values compared to those measured in the experiment. It is obvious from fig. 4 that the selected velocity also produces unsatisfactory results, the maximal temperature is much higher and cooling time is much lower than measured in the experiment.

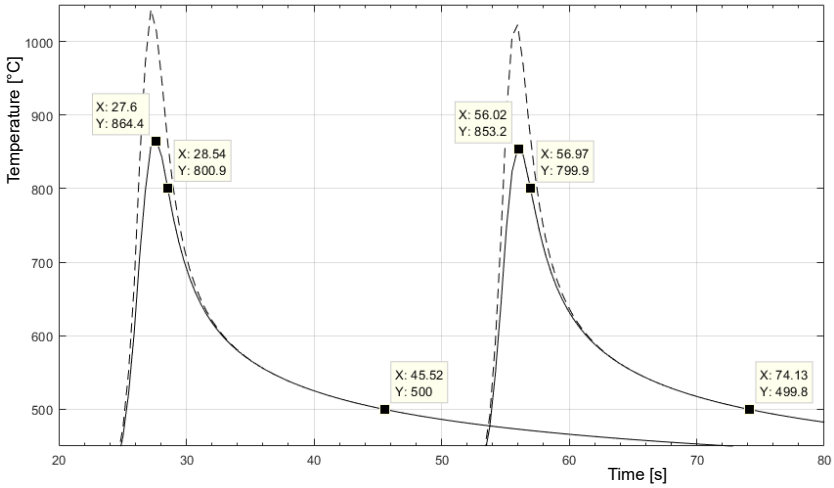

Figure 4. Numerical results for the temperature as a function of time from 450 °C for the point in the symmetry plane (y = 0), at x = 0.1 m, x = 0.2 m, and z = 0.003 m and 0.004 m (intended for the case where heat input is 16736 J/cm and electrode diameter 5 mm)

The same behavior is observed in the case carried out on the plate of 20 mm thickness and initial temperature of 20 °C, tab. 2, No. 3. Results are presented in fig. 5.

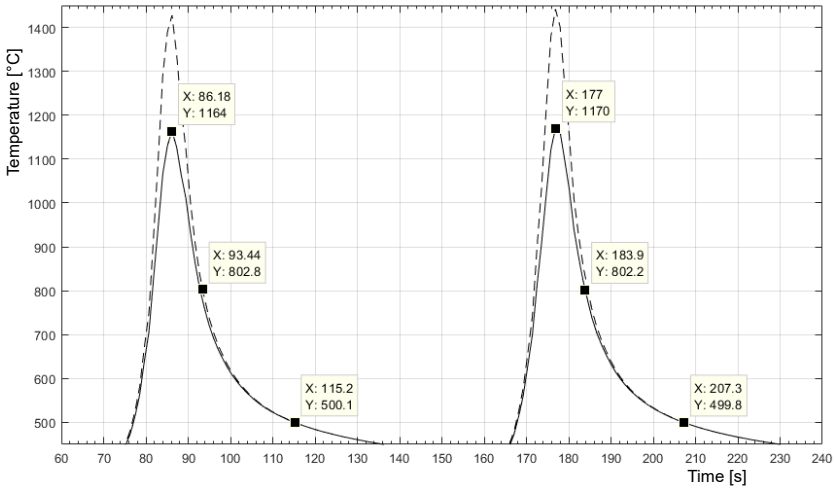

Figure 5. Numerical results for the temperature as a function of time from 450 °C for the point in the symmetry plane (y = 0), at x = 0.1 m, x = 0.2 m, and z = 0.003 m and 0.004 m (heat input is 48610 J/cm and electrode diameter 5 mm)

The velocity of the heat source was 0.0011 m/s. The experimentally measured cooling time was 28 seconds and numerically calculated time was around 22 seconds while the calculated maximal temperature was 20 °C higher than measured.

Final example was the plate of 30 mm thickness and initial temperature of 97 °C. The selected velocity of the heat source was 0.0015 m/s, fig. 6. The maximal temperature was again higher than measured. The values of cooling time were higher than experimentally measured but lower than value obtained using the Japanese authors formula, tab. 2, No. 2.

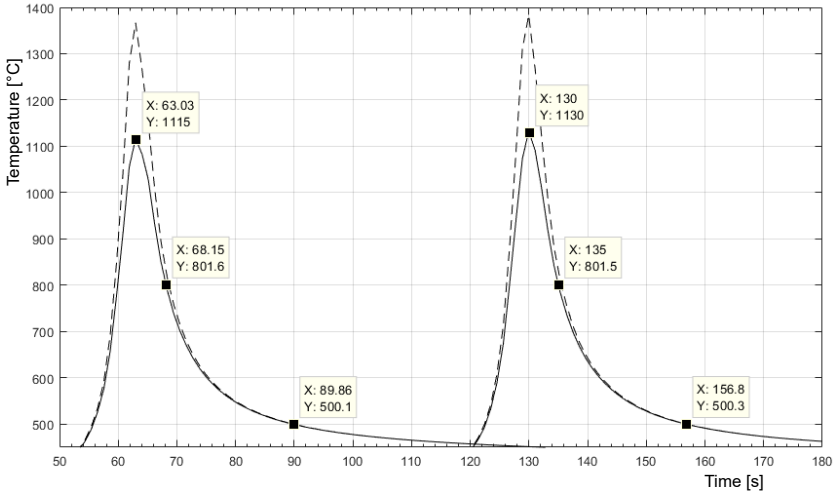

Figure 6. Numerical results for the temperature as a function of time from 450 °C for the point in the symmetry plane (y = 0), at x = 0.1 m, x = 0.2 m, and z = 0.003 m and 0.004 m (heat input is 38667 J/cm and electrode diameter 5 mm)

Conclusions

The aim of this research was to determine temperature cycles during hard facing of carbon steels in order to determine cooling time between 800 ºC and 500 ºC. After experiment, the FEM analysis with same input parameters was done and the obtained results were compared to one obtained by empirical formulas and welding recommendations.

Based on conducted experimental and numerical investigation it can be concluded that the correlation of numerical results to experimental ones is very good, especially when compare heating and cooling part of curves, what was aim of the research. The time between 800 ºC and 500 ºC was almost as experimental in every analyzed case. Numerical thermal cycle's curves show a little bit higher maximal temperatures so that cause deviation of experimental curves, but it must be noted that the presented model is not appropriate for determination of this parameter since it was developed for analysis of cooling time in different temperature range (800-500 ºC). Presented research confirmed the possibilities to use FEM simulations in order to shorten the time needed for determination of optimal welding technologies and possible prediction of structures in zone of hard facing or welding.

Nomenclature

a, b, c – parameters of the semi-axis of the ellipsoid
d_e – electrode diameter, [mm]
f_f – front values of the parameter
f_r – rear values of the parameter
I – welding current, [A]
Q – power, [W]
$q(x, y, z, t)$ – heat source, [J]
q_l – heat input [Jcm^{-1}]
T_0 – initial temperature, [ºC]
T_{max} – maximal temperature, [ºC]
$t_{8/5}$ – cooling time, [s]
U – welding voltage, [mm]
v_s – welding velocity, [cms^{-1}]
x_0 – initial position of the heat source

Acknowledgement

This research was partially financially supported by the Ministry of Education and Science of Republic of Serbia through grant TR35024.

References

[1] Arsić, D., *et al.,* Selection of the Optimal Hard Facing (HF) Technology of Damaged Forging Dies Based on Cooling Time $t_{8/5}$, *Metalurgija - Metallurgy*, *55* (2016), 1, pp. 103-106
[2] Arsić, D., *et al.,* Impact of the Hard-Facing Technology and the Filler Metal on Tribological Characteristics of the Hard-Faced Forging Dies, *Tehnički Vjesnik - Technical Gazette*, *22* (2015), 5, pp. 1353-1358
[3] Sedmak, A., *et al.,* Experimental and Analytical Evaluation of Preheating Temperature During Multipass Repair Welding, *Thermal Science*, *21* (2017), 2, pp. 1003-1009
[4] Lazić, V., *et al.,* Reparation of the Damaged Forging Hammer Mallet by Hard Facing a Weld Cladding, *Technical Gazette*, *16* (2009), 4, pp. 107-113
[5] Chen, W. J., *et al.,* Microstructure and Fatigue Crack Growth of EA4T Steel in Laser Cladding Remanufacturing, *Engineering Failure Analysis*, *79* (2017), Sept., pp. 120-129
[6] Abbas, R., A Review on the Wear of Oil Drill Bits (Conventional and the State of the Art Approaches for Wear Reduction and Quantification), *Engineering Failure Analysis*, *90* (2018), Aug., pp. 554-584
[7] Lazić, V., *et al*., Reparation By Hard Facing of the Damaged Secondary Stone Crushers, *Manufacturing Technology, 16* (2016), 2, pp. 375-380
[8] Lazić, V., *et al.,* Techno-Economic Justification of Reparatory Hard Facing of Various Working Parts of Mechanical Systems, *Tribology in Industry*, *36* (2014), 3, pp. 287-292
[9] Đurđević, A., *et al.,* Numerical Analysis of Heat Transfer During Friction Stir Welding, *Structural Integrity and Life, 17* (2017), 1, pp. 45-48
[10] Lazic, V., *et al.,* Theoretical-Experimental Determining of Cooling Time ($t_{8/5}$) in Hard Facing of Steels for Forging Dies, *Thermal Science*, *14* (2010), 1, pp. 235-246

[11] Kumar, A., *et al.,* Thermo-Mechanical Behaviour of Microstretch Thermoelastic Medium with Microtemperatures Subjected to Input Heat Source, *Structural Integrity and Life*, *18* (2018), 2, pp. 121-127
[12] Meseguer-Valdenebro, J. L., *et al.,* Calculation of $t_{8/5}$ by Response Surface Methodology for Electric Arc Welding Applications, *Thermal Science*, *18* (2014), Suppl. 1, pp. S149-S158
[13] Gadallah, R., *et al.,* Critical Investigation on the Influence of Welding Heat Input and Welding Residual Stress on Stress Intensity Factor and Fatigue Crack Propagation, *Engineering Failure Analysis*, *89* (2018), July, pp. 200-221
[14] Lazić, V., *et al.,* Evaluation of Expressions for Calculating the Cooling Time in Carbon Steels Welding, *Proceedings*, 3rd International Conference on Advances and Trends in Engineering Sciences and Technologies, 2018, Tatranske Matliare, Slovakia, pp. 179-184
[15] Lazić, V., *et al.,* Numerical Analysis of Temperature Field During Hard-Facing Process and Comparison with Experimental Results, *Thermal Science*, *18* (2014), Suppl. 1, pp. S113-S120
[16] Sedmak, S., *et al.,* Numerical Analysis of Different Weld Geometries of Lap Welded Joint in Ammonia Transport Tanks, *Structural Integrity and Life*, *17* (2017), 3, pp. 217-220
[17] Vetriselvan, R., *et al.,* Experimental and Numerical Investigation on Thermal Fatigue Behaviour of 9Cr1Mo Steel Tubes, *Engineering Failure Analysis*, *84* (2018), Feb., pp. 139-150
[18] Cvetkovski, S., *et al.,* Welding Heat Input Determination in TIG and Laser Welding of LDX 2101 Steel by Implementing the Adams Equation for 2-D Heat Distribution, *Structural Integrity and Life*, *10* (2010), 2, pp. 103-109
[19] Kalaba, D., *et al.,* Thermomechanical Modeling the Resistance Welding of PbSb Alloy, *Thermal Science, 14* (2010), 2, pp. 437-450
[20] Perret, W., *et al.,* Comparison of Analytical and Numerical Welding Temperature Field Calculation, *Computational Materials Science, 47* (2010), 4, pp. 1005-1015
[21] Meseguer-Valdenebro, J. L. M., *et al.,* Numerical-Experimental Validation of the Welding Thermal Cycle Carried Out with the MIG Welding Process on a 6063-T5 Aluminium Tubular Profile, *Thermal Science, 23* (2019), 6A, pp. 3639-3650
[22] Nejković, V. M., *et al.,* New Method for Determining Cooling Time and Preheating Temperature in Arc Welding, *Thermal Science, 23* (2019), 6B, pp. 3975-3984
[23] Vukićević, M., *et al.,* Analytical Algorithm Expressions in Simulation of the Temperature Field in Electric Resistance Spot Welding, *Technical Gazette*, *25* (2018), 1, pp. 64-71
[24] Perić, M., *et al.,* A Simplified Engineering Method for a T-Joint Welding Simulation, *Thermal Science*, *22* (2018), Suppl. 3, pp. S867-S873
[25] Goldak, J., *et al.,* A New Finite Element Model for Welding Heat Sources, *Metallurgical Transactions B*, *15* (1984), 2, pp. 299-305
[26] Smith, M. C., Smith, A. C., NeT Bead-on-Plate Round Robin: Comparison of Transient Thermal Predictions and Measurements, *International Journal of Pressure Vessels and Piping, 86* (2009), 1, pp. 96-109
[27] Pahkamaa, L., *et al.,* A Method to Improve Efficiency in Welding Simulations for Simulation Driven Design, *Proceedings,* ASME 2010 International Design Engineering Technical Conference & Computers and Information in Engineering Conference IDETC/CIE 2010, Montreal, Canada, 15-18 August, 2010, Vol. 3, pp. 81-90
[28] Goldak, J., *et al.,* Why Power Per Unit Length of Weld Does not Characterize a Weld, *Computational Materials Science, 48* (2010), 2, pp. 390-401
[29] Veljic, D., *et al.,* Numerical Simulation of the Plunge Stage in Friction Stir Welding, *Structural Integrity and Life, 11* (2011), 2, pp.131-134
[30] Atanasovska, I., *et al.,* Coupled Nonlineary Problems in Finite Element Analysis – A Case Study, *Structural Integrity and Life, 12* (2012), 3, pp. 201-208
[31] Ivanović, I., *et al.,* Numerical Study of Transient Three-Dimensional Heat Conduction Problem with a Moving Heat Source, *Thermal Science*, *15* (2011), 1, pp. 257-266
[32] Tavares, S. S. M., *et al.,* Failure of Super 13Cr Stainless Steel Due to Excessive Hardness in the Welded Joint, *Engineering Failure Analysis*, *91* (2018), Sept., pp. 92-98
[33] Wang, Y., *et al.,* Jagged Cracking in the Heat-Affected Zone of Weld Overlay on Coke Drum Cladding Overlay Panel, *Engineering Failure Analysis*, *85* (2018), Mar., pp. 14-25
[34] Jeremić, L., *et al.,* Effect of Plasma Hardfacing and Carbides Presence on the Occurrence of Cracks and Microcracks, *Structural Integrity and Life*, *18* (2018), 2, pp. 99-103

[35] Tanasković, D., *et al.,* Cracking Due to Repair Welding of the Treiber Roll, *Structural Integrity and Life*, *17* (2017), 2, pp. 133-138
[36] ***, EN 10025-2: Hot Rolled Products of Structural Steels – Part 2: Technical Delivery Conditions for Non-Alloy Structural Steels
[37] ***, Code Aster, *Documentation version 11*, Online Version Available at: www.code-aster.org.

Paper submitted: July 17, 2019
Paper revised: August 25, 2019
Paper accepted: August 31, 2019